Geoderma 451 (2024) 117084

Contents lists available at ScienceDirect

Geoderma

journal homepage: www.elsevier.com/locate/geoderma

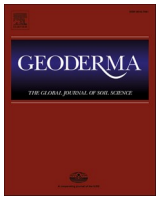

# Impact of a synthetic zeolite mixed with soils of different pedological characteristics on soil physical quality indices

Antonio Satriani [a,*], Claudia Belviso [a], Stella Lovelli [b], Simone di Prima [b], Antonio Coppola [c], Shawkat B.M. Hassan [b], Anna Rita Rivelli [b], Alessandro Comegna [b]

[a] National Research Council-Institute of Methodologies for Environmental Analysis, Tito Scalo, PZ, Italy
[b] Department of Agricultural, Forest, Food and Environmental Sciences, University of Basilicata, Potenza, Italy
[c] Department of Chemical and Geological Sciences, University of Cagliari, Italy

ARTICLE INFO

Handling Editor: Jingyi Huang

*Keywords:*
Field capacity
Soil water retention curves
Soil pore size distribution
Integral energy
Synthetic zeolite

ABSTRACT

The addition of natural or synthetic zeolites induces changes in a soil's chemical, physical, and biological characteristics. Zeolites possess intricate internal frameworks that allow them to modify soil structure and texture, thereby impacting soil hydrological properties. This potential offers opportunities to control soil and groundwater pollution as well as optimize irrigation management practices. In this study, three sandy-loam soils and a silty-loam soil were collected and mixed with different amounts of synthetic zeolite derived from coal fly ash. Repacked soil samples were combined with four levels of zeolite ranging from 1% to 10% by weight and were then hydraulically characterized. This included measuring soil water retention curves (SWRCs) of soil-zeolite mixtures. The data revealed, in accordance with recent research findings, that zeolite influences the hydraulic behavior of soils. In general, we observed that, as the percentage of zeolite increases in the soil, the SWRCs are shifted upwards. This effect is fundamental for explaining the observed changes in the whole set of investigated soil hydraulic properties. The observed changes are also fundamental to evaluate selected soil physical quality (SPQ) indices of agronomic interest, which are investigated in depth in the present research. A specific focus was on the impact of zeolite on modifying the soil's capacity to retain water, hence on the energy required by plants to acquire a unit mass of soil water (referred to as integral energy, $E_I$). Finally, the ANOVA test, linear regression, and multivariate analysis were performed on the entire dataset to support, from a statistical standpoint, the observed correlations between SPQ indices and zeolite amounts. These findings underscored the significance of soil texture in selecting the appropriate soil type for zeolite amendment, confirming that coarse-textured soils are more suitable for zeolite treatment compared to fine-textured soils.

## 1. Introduction

The intricate interplay between soil chemical and physical properties forms the foundation for understanding their behavior and functions within the broader environmental context. Chemical composition, influenced by mineral content and organic matter, deeply impacts nutrient availability, soil acidity, and microbial activity (Six et al., 2002; Dexter, 2004; Comegna et al., 2013; Zheng et al., 2019; Ndung'u et al., 2021). On the other hand, soil physical characteristics, including texture, structure, and water retention capacity, dictate water movement, aeration, and root penetration. The synergy between these chemical and physical attributes shapes the soil's ability to support plant life and plays a pivotal role in several environmental processes. In essence, exploring the dynamic interaction among these attributes reveals the complex fabric of the soil ecosystem, providing essential insights for sustainable land use, agriculture, and ecosystem management (Dexter, 1988; Dexter et al., 2008; Guber et al., 2003; Novotny et al., 2023, among others). From an agricultural perspective, a soil's physico-chemical properties significantly impact crop development, and to obtain crop yield performance with high water use efficiency, *good soil quality* is required. Changes in a soil's physico-chemical properties are analyzed by examining the variations in the pore size distribution (PSD) and water retention curve (SWRC) through the van Genuchten model (van Genuchten, 1980).

The concept of soil physical quality (SPQ) indicators, through the indicators of air capacity (AC), available water content (AWC), relative

* Corresponding author.
*E-mail address:* antonio.satriani@cnr.it (A. Satriani).

https://doi.org/10.1016/j.geoderma.2024.117084
Received 16 April 2024; Received in revised form 22 October 2024; Accepted 22 October 2024

field capacity (RFC), macroporosity ($V_{mac}$) and microporosity ($V_{mic}$), among others, was introduced by Topp et al. (1997), Dexter and Bird (2001), Dexter (2004), and Reynolds et al. (2002), Reynolds et al. (2008), Reynolds et al. (2009). In agronomic contexts, this concept is particularly helpful for quantifying the degree of soil quality and thus developing *best management* land use practices, that can be used to maximize crop performance (Mueller et al., 2008; Drewry et al., 2008). The concept is usually applied by identifying one or more soil properties as indicators of soil physical quality and establishing optimal ranges for the selected indicators (Reynolds et al., 2008).

Reynolds et al. (2007) highlighted the correlation between RFC and AC as an indicative measure of soil quality, delineating a range of optimal values and critical limits. The optimal balance between water content and air content in the soil provides insights into the soil's ability to store and adequately supply water, air, and nutrients. This physical quality indicator is influenced by the soil pore size distribution (Reynolds et al., 2002; Dexter, 2004) and is closely linked to the concept of available water content.

The simplified approach of Veihmeyer and Hendrickson (1927), asserting that water is uniformly available to crops within a specific range of values for a given soil, introduced the concept of AWC. This basic idea of water availability within the interval defined by an upper limit termed field capacity (FC) and a lower limit, namely permanent wilting point (PWP), was introduced to guide irrigation management. FC is defined as the soil water content corresponding to the full saturation of the micropores after the gravitational water in the macropores has drained away (Veihmeyer and Hendrickson, 1931), while PWP is defined as the soil water content at which conventionally plants irreversibly wilt. AWC is divided into two components: readily available water content (RAWC) and non-readily available water content (NRAWC). The RAWC and NRAWC components represent the soil moisture content between FC and a stress point or "refill point" and between this stress point and PWP, respectively. These parameters are essential for assessing soil water storage and are widely utilized in irrigation scheduling (Drewry et al., 2008; Reynolds et al., 2009; Fu et al., 2021). Efficient irrigation scheduling optimizes water application at the right times and volumes, and FC represents the threshold storage to control the optimal irrigation amount by limiting underwatering or overwatering (Nasta et al., 2023).

There is no uniformity in the determination of the soil moisture value corresponding to FC. Several authors have proposed static criteria with fixed values of matric potential ($\psi$) associated with FC. A commonly used value of FC is the soil water content at a matric potential of − 33 kPa or − 10 kPa (Richards and Weaver, 1944; Colman, 1947; Romano and Santini, 2002) or − 6 kPa (Villagra-Mendoza et al., 2021). According to some authors (Hillel, 1980, 1998; Meyer and Gee, 1999; Ahuja et al., 2008), these benchmark pressures do not ensure that the drainage would become negligible. Therefore, several researchers have considered dynamic approaches based on the attainment of a negligible drainage flux, proposing that the soil's FC corresponds to the soil water when the drainage flux from the soil reaches a value of 0.01 cm $d^{-1}$ (Hillel, 1998; Meyer and Gee, 1999; Dirksen and Matula, 1994; Twarakavi et al., 2009).

Assouline and Or (2014) proposed an alternative dynamic criterion based on the soil water release curve to estimate the matric potential value at field capacity ($\psi_{FC}$) which causes the loss of hydraulic continuity and produces negligible drainage. In this case, the size distribution of the hydraulically connected pores determines $\psi_{FC}$.

The correlation between AWC and plant growth is significant. However, selecting a specific criterion for establishing the FC not only affects the determination of AWC but also other indicators of soil quality. Additionally, plant water uptake is influenced by the potential evaporation rate and rooting density. Hence, a novel concept has been introduced, considering the energy required by the plant to absorb water from the soil (Asgarzadeh et al., 2011; Chamindu Deepagoda et al., 2013; Barati et al., 2015) by using the integrated area under the SWRC.

Minasny and McBratney (2003) introduced the concept of integral energy ($E_I$) to measure the amount of energy needed by plants to absorb a unit of water from the soil within a specific range of water content or matric potential. They determined this energy by calculating a definite integral of the SWRC. The study conducted by Minasny and McBratney (2003) found that soils with similar AWC may exhibit different SWRCs, resulting in different $E_I$ values.

The application of various soil amendments, such as bentonite, hydrogel, silica, biochar, and zeolite, has gained increasing interest in agriculture due to their environmentally friendly nature and their ability to enhance water availability. This growing interest is driven by environmental concerns and the limited water resources in arid and semi-arid regions, such as the Mediterranean area (Demitri et al., 2013; Satriani et al., 2018; Mohawesh and Durner, 2019; Saha et al., 2020; Villagra-Mendoza et al., 2021). The greater mobility of water in amended soil as it dries allows plants to access more water compared to unamended soil (Schaller et al., 2020; Zarebanadkouki et al., 2022).

In recent years, the use of zeolites in agriculture has been extensively discussed (Cataldo et al., 2021), especially their effect on saturated hydraulic conductivity (Jakkula and Wani, 2018), soil infiltration rate (Szerement et al., 2014), soil water content and water retention capacity (Ravali et al., 2020; Comegna et al., 2023), and soil quality in different agricultural management systems (Ferretti et al., 2024). Zeolites are a group of natural and synthetic crystalline aluminosilicates with a framework of linked $TO_4$ tetrahedra (where T = Si, Al, or others), each consisting of four oxygen atoms surrounding a cation. The three-dimensional networks containing cavities and channels impart a large surface area and porosity to these minerals, and are characterized by a high-level cation exchange capacity (CEC). Due to their high CEC and high water adsorption, zeolites have been used in agriculture (Elliot and Zhang, 2005; Cobzaru and Inglezakis, 2012; Nakhli et al., 2017; Jarosz et al., 2022). For example, in sandy soils and loamy soils, zeolite addition has the effect of increasing soil water retention and water holding capacity and reducing hydraulic conductivity at saturation and infiltration rate (Colombani et al., 2015). Further, a recent study conducted by Comegna et al. (2023) showed that the addition of zeolites alters soil properties due to changes in the original pore size distribution (PSD) with an effect on the SWRC shape and hence on the AWC and soil hydraulic conductivity.

In this study, we selected four soils of different textures and pedological characteristics. Our main objectives were to: i) estimate a series of soil physical quality parameters of agronomic interest in soils mixed with different amounts of a synthetic zeolite, ii) explore the possible correlations among the chosen SPQ properties as a function of zeolite content, iii) evaluate the impact of different selected criteria for determining FCs on the selected SPQ indicators, and iv) use the obtained structural regression to infer soil-zeolite specific optimal ranges for selected soil physical quality indicators.

## 2. Materials and methods

### 2.1. Soil and zeolite characterization

A series of laboratory experiments were conducted using repacked soil samples collected from the $A_p$ horizon of four soil sites located in the Basilicata region (Italy), hereafter referred to as Genzano (G), Metaponto (M), Rapolla (R), and Pignola (P) soils (Fig. 1).

Soil samples were dried at 105 °C, passed through a 2-mm sieve, and finally mixed with four zeolite percentages by weight: 1 % (Z1), 2 % (Z2), 5 % (Z5), and 10 % (Z10). For each soil, a repacked soil sample, without zeolite (labeled Z0), was prepared and used as a reference. Overall, 60 soil samples (5 samples × 3 replicates for each soil), each measuring 110 mm in length and 80 mm in diameter, were prepared and tested.

The main physico-chemical soil properties are displayed in Table 1 (see also Comegna et al., 2023 for more details). In particular, soil


**Fig. 1.** Map location of the four field sites in Basilicata (Italy).

texture, bulk density ($\rho_b$), and pH were determined using the methods proposed by Day (1965), Blake and Hartge (1986), and Eckert (1988), respectively. The soil samples were amended with zeolite synthesized from fly ash as described in Belviso et al. (2022). Fly ash is a waste resulting from coal combustion in thermo-electric power plants (Belviso, 2018). A comprehensive characterization of the zeolite sample is provided in the Supplementary Material.

### 2.2. Measurements of soil hydraulic properties in soil–zeolite mixtures

The experimental soil water retention curve was obtained on each soil sample by using the hanging water column method (Stackman et al., 1969; Dane and Hopmans, 2002). Specifically, for each soil, SWRCs were determined on 5 × 3 column replicates. Experimental SWRC values were obtained in the matric potential ($\psi$) range from 0 to 25 kPa.

The experimental soil water retention curves obtained from laboratory tests were then modeled using the van Genuchten equation (vG; van Genuchten, 1980):

$$\theta = \theta_r + \frac{\theta_s - \theta_r}{[1 + \alpha|\psi|^n]^m} \quad (1)$$

where θ ($cm^3/cm^3$), $\theta_s$ ($cm^3/cm^3$), and $\theta_r$ ($cm^3/cm^3$) are the volumetric water content, the volumetric water content at saturation, and the residual volumetric water content, respectively; $n$ (−), $m$ (=1–1/$n$), and $\alpha$ are shape parameters. The RETC optimization software package (van Genuchten et al., 1991) was used to estimate the van Genuchten parameters.

Furthermore, on the same soil-zeolite mixtures, the normalized pore-size distribution (PSD) functions (obtained by differentiating Eq. (1) with respect to $\psi$ and by dividing each PSD by the PSD function at the inflection point) were also determined (Durner, 1994; Coppola, 2000; Dexter, 2004; Jensen et al., 2019):

$$S^*(\psi) = \frac{m(\alpha|\psi|)^n[1 + m^{-1}]^{(m+1)}}{[1 + (\alpha|\psi|)^n]^{(m+1)}}, 0 \le S_h^* \le 1 \quad (2)$$

Note that $S^*(\psi)$ is independent of bulk density and porosity, which is useful for comparing PSDs among different porous materials.

Furthermore, a series of parameters, which characterize the PSD function that are: i) the modal ($d_{mode}$), ii) median ($d_{median}$), and iii) mean equivalent pore diameter ($d_{mean}$) values (named "location" parameters and expressed in μm; Reynolds et al., 2009; dos Reis et al., 2019), as well as iv) the standard deviation ($SD$), v) skewness ($Skw$), and vi) kurtosis ($Kurt$), (named "shape" parameters, dimensionless), were determined using the following equations (Reynolds et al., 2009; Blott and Pye, 2001):

$$d_{mode} = \frac{2980\alpha}{m^{\frac{-1}{n}}} \quad (3)$$

$$d_{median} = \frac{2980\alpha}{\left(0.5^{-\frac{1}{m}} - 1\right)^{\frac{1}{n}}} \quad (4)$$

$$d_{mean} = exp\left(\frac{lnd_{0.16} + lnd_{0.50} + lnd_{0.84}}{3}\right) \quad (5)$$

$$SD = exp\left(\frac{lnd_{0.84} - lnd_{0.16}}{4} + \frac{lnd_{0.95} - lnd_{0.05}}{6.6}\right) \quad (6)$$

$$Skw = \frac{1}{2}\left[\frac{lnd_{0.16} + lnd_{0.84} - 2(lnd_{0.50})}{lnd_{0.84} - lnd_{0.16}} + \frac{lnd_{0.05} + lnd_{0.95} - 2(lnd_{0.50})}{lnd_{0.95} - lnd_{0.05}}\right] \quad (7)$$

$$Kurt = \frac{lnd_{0.05} - lnd_{0.95}}{2.44(lnd_{0.25} - lnd_{0.75})} \quad (8)$$

where $d_i$ values ($i$ = 0.05, 0.16, 0.25, 0.50, 0.75, 0.84 and 0.95) are cumulative percentile values that is the grain size at which a specified percentage of the grains are coarser (Blott and Pye, 2001). Finally, saturated hydraulic conductivity ($K_s$) was also measured on the whole set of soil-zeolite mixtures using the constant head method (Klute and Dirksen, 1986; Coppola et al., 2019).

### 2.3. Estimation of soil water storage parameters

FC, AWC, RAWC, RFC, and $E_I$ are key parameters of agronomic interest, that are widely used as indicators of the soil suitability for crop growth.

**Table 1**
Principal physico-chemical properties and pedological classification (IUSS Working Group WRB, 2006) of the investigated soils.

| Soils | Soil texture and classification (USDA) | | | | Soil pedological classification | $\rho_b$ (g $cm^{-3}$) | pH |
|---|---|---|---|---|---|---|---|
| | Texture | Sand (%) | Silt (%) | Clay (%) | | | |
| Genzano (G) | Sandy-loam | 57.43 | 31.95 | 10.62 | Luvic Kastanozems | 1.15 | 7.7 |
| Metaponto (M) | Sandy-loam | 53.81 | 34.94 | 11.25 | Eutric Vertisols | 1.10 | 7.9 |
| Rapolla (R) | Sandy-loam | 59.89 | 28.86 | 11.25 | Eutric Cambisol | 1.14 | 7.2 |
| Pignola (P) | Silty-loam | 9.53 | 66.18 | 24.29 | Epileptic Phaeozems | 1.13 | 7.6 |

In the present research, since there is no uniformity regarding the criteria for FC determination, four different FC values were calculated following two static and two dynamic criteria. With regard to static criteria, FC was considered the water content at a matric potential ($\psi$) of − 10 ($FC_{10}$) and − 33 kPa ($FC_{33}$). For the dynamic approach, the field capacity (termed $FC_{dyn}$) was considered the water content when the drainage flux from the soil reached a value of 0.01 cm $d^{-1}$ (Hillel, 1998; Meyer and Gee, 1999; Dirksen and Matula, 1994; Twarakavi et al., 2009), while using the Assouline and Or (2014) approach, the soil matric potential ($\psi$) at FC (termed $FC_{AO}$) derives from drainable soil pore size distribution to characterize the loss of hydraulic continuity inside the soil pores which results in negligible drainage (Assouline and Or, 2014). In both adopted criteria, FC is expressed as the ratio of the volume of water to the unit volume of soil.

To estimate $FC_{dyn}$ and $FC_{AO}$ the following equations from Twarakavi et al. (2009) and Assouline and Or (2014) were used (setting the residual water content $\theta_r = 0$):

$$\theta_{FC_{dyn}} = \theta_s\left(n^{-0.60(2+log(K_s))}\right) \tag{9}$$

$$\theta_{FC_{AO}} = \theta_s\left\{1+\left[\left(\frac{n-1}{n}\right)^{(1-2n)}\right]\right\}^{\left(\frac{1-n}{n}\right)} \tag{10}$$

Using the four FC definitions, the following soil water storage parameters were determined: i) AWC (equal to the difference between θ at FC and permanent wilting point PWP, the latter defined as θ at $\psi = -1500$ kPa, ii) RAWC (equal to the difference between θ at FC and θ at $\psi = -100$ kPa; Houlbrooke and Laurenson, 2013; Fu et al., 2021).This difference corresponds approximately to water stored in pores sized between 30 and 3 μm if $FC_{10}$ is considered, between 9 and 3 μm for $FC_{33}$, and between 50 and 3 μm for $FC_{dyn}$ and $FC_{AO}$ (Jensen et al., 2019), iii) RFC (which indicates the soil's ability to store water and air; Reynolds et al., 2008):

$$RFC = \left(\frac{\theta_{FC}}{\theta_s}\right) = \left[1-\left(\frac{AC}{\theta_s}\right)\right] \tag{11}$$

where AC is soil air capacity (equal to $\theta_s$-$\theta_{FC}$), and iv) the integral energy ($E_I$), expressed in Joule $kg^{-1}$ (Minasny and McBratney 2003):

$$E_I\left[\theta_{init}-\theta_{final}\right] = \frac{1}{10\left(\theta_{init}-\theta_{final}\right)}\int_{\theta_{final}}^{\theta_{init}}\psi(\theta)d\theta \tag{12}$$

where $\theta_{init}$ is θ at FC, while $\theta_{final}$ is θ at PWP and at $\psi = -100$ kPa, and the interval $\left(\theta_{init}-\theta_{final}\right)$ denotes the volumetric water content domain of AWC or RAWC (with *init* > *final*). $E_I$ calculations were done using Wolfram Alpha computational software (Oxford, UK), while the SAWCal software (Asgarzadeh et al., 2014) was used to verify the correctness of the calculation of the $E_I$ values.

### 2.4. Statistical analysis

The experimental data were analyzed using SPSS software (IBM, SPSS Statistic for data analysis, IBM Corp., NY, USA). Before performing the analysis of variance (ANOVA), the Shapiro-Wilk ($p \leq 0.05$) and the Levene ($p \leq 0.05$) tests were applied to test normality and homogeneity of variances, respectively. Subsequently, FC, AWC, RAWC, RFC, and $E_I$ estimated values were compared, for a fixed soil, among the selected zeolite treatments by one-way analysis of variance (ANOVA). The differences between means were compared using the HSD Tukey's test at the significance level of $p \leq 0.05$. $FC_{dyn}$ and $FC_{AO}$, AWC, $E_I[\theta AWC_{AO}]$ and $E_I[\theta AWFC_{10}]$ were subjected to logarithmic transformation to achieve the normality distribution. Multiple stepwise linear regression analysis of RFC and $E_I$ on the vG model parameters and soil pore parameters was carried out to identify the best predictors. A multivariate analysis using principal component analysis (PCA) and cluster analysis (CA) was performed to reduce the investigated variables and classify the soils that respond to internal homogeneity criteria. Because the variables were in differing scales, a *z*-score standardization was performed. Before performing the PCA, the Kaiser-Meyer-Olkin (KMO) test and Bartlett's test of sphericity were used. The first test measures the sampling adequacy for PCA and the second whether there is a correlation between the variables.

Moreover, the analysis involved a combination of hierarchical and non-hierarchical cluster analysis. The hierarchical method was used first to determine the exact number of clusters, using the complete linkage cluster method and squared Euclidean distance. Once the number of clusters had been identified, non-hierarchical *K*-means cluster analysis was applied. The ANOVA test within the *K*-means procedure helped identify which variables contributed most to identifying the clusters. Finally, the output of the K-means method was presented in the form of a clustered bar graph.

## 3. Results and discussion

### 3.1. Effects of zeolite on soil physical quality indices

The effects of zeolite on the whole SWRC shape may be observed in Fig. 2a, b, c, d, showing, for each soil and zeolite treatment, the experimental SWRCs modeled with Eq. (1). Our data revealed that zeolite affects the whole SWRC shape. In general, as a first approximation, it can be observed that as the percentage of zeolite increases in the soil, the SWRCs shift upwards. This effect is evident in all the soil-zeolite mixtures.

Related to the figures above, Table 2 reports a synthesis of the α and *n* vG model parameters and the coefficient of determination $R^2$ (which expresses the goodness of fit between measured SWRCs and those modeled with equation (1), as well as the calculated values of $\theta_s$, $K_s$, θ, and Ψ at the inflection point (called $\theta_i$ and $\Psi_I$ respectively).

As reported by Dexter (2004) and Jensen et al. (2019), the change in the size of the predominant pores ($d_{mode}$) occurs at the inflection point, increasing the proportion of smaller pores at matric potential over the inflection point. Following the approaches of Dexter and Bird (2001), the inflection point corresponds to the optimum for soil tillage.

Fig. 3 shows the normalized PSD functions. The different soil-zeolite combinations exhibit similar shapes and positions, especially for the sandy-loam soils of G, M, and R. In the silty-loam soil of P, the zeolite effect is less evident (in terms of normalized PSD) but not negligible at higher contents (i.e., 5 % and 10 %; see also Comegna et al., 2023). Overall, the selected synthetic zeolite exhibited a dual effect on soils, modifying their original structure, with a particular impact on the macropore region, as well as on the meso- and micro-pore regions, which increased due to the high micropore volume of the zeolite. The latter effect gradually shifts the peak of normalized PSDs from larger to narrower pores (Szatanik-Kloc et al., 2021; Ibrahim and Alghamdi, 2021).

Table 3 illustrates a selection of some location and shape parameters related to the PSD curves. On average, in all soils, the increase in the amount of zeolite results in a reduction of the location parameter values.

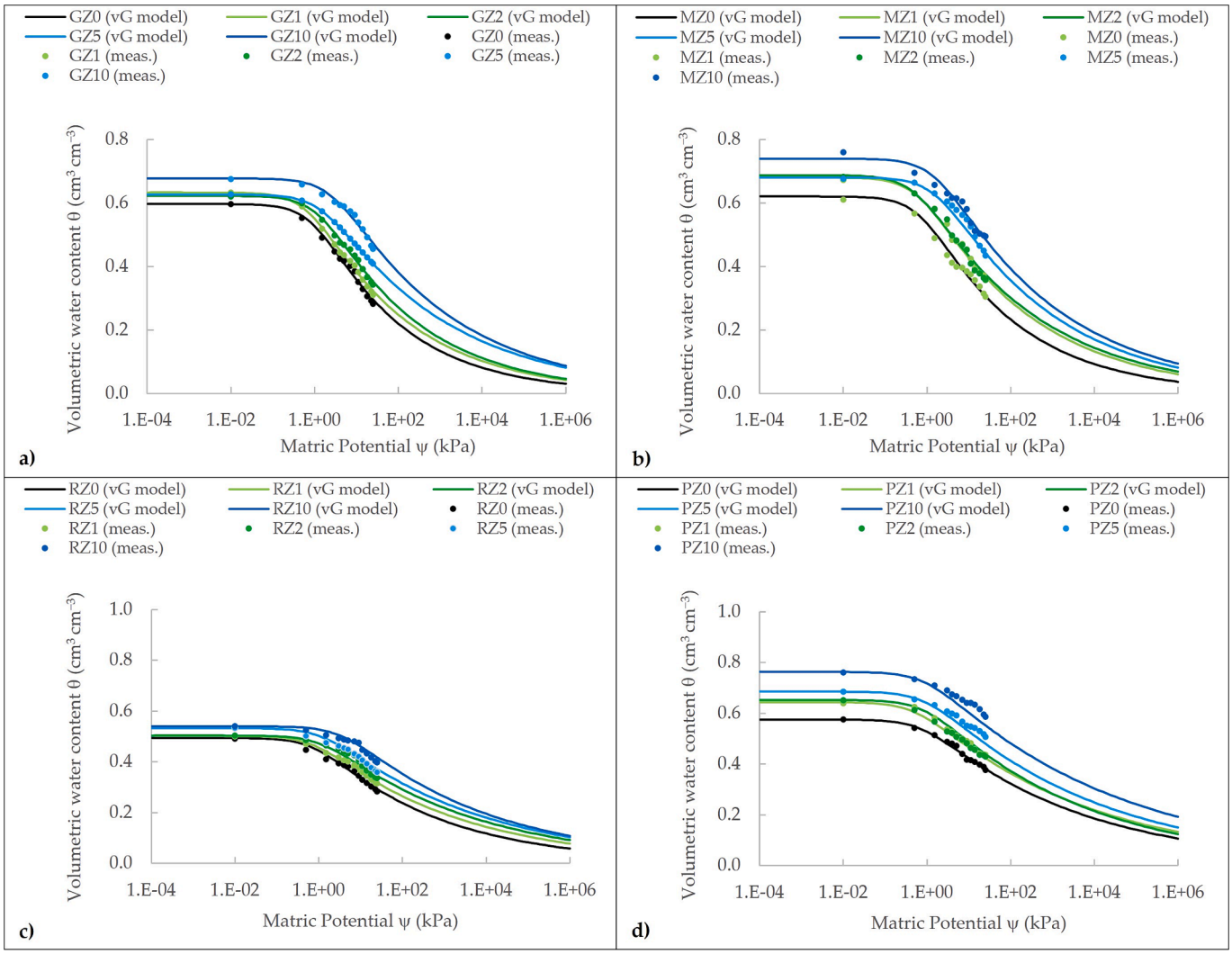


**Fig. 2.** SWRCs modeled by the vG equation concerning the selected soils: a) Genzano (G), b) Metaponto (M), c) Rapolla (R), d) Pignola (P), and soil-zeolite mixtures (Z0, Z1, Z2, Z5, and Z10).

**Table 2**
Volumetric water content at saturation ($\theta_s$), saturated hydraulic conductivity ($K_s$), volumetric water content ($\theta_i$) at inflection point, and matric potential ($\Psi_i$) at inflection point; vG model parameters $\alpha$ and $n$, and coefficient of determination $R^2$.

| Soil | Zeolite treatment | $\theta_s$ (cm$^3$ cm$^{-3}$) | $K_s$ (cm min$^{-1}$) | $\theta_i$ (cm$^3$ cm$^{-3}$) | $\Psi_i$ (kPa) | $\alpha$ (cm$^{-1}$) | $n$ (–) | $R^2$ |
|---|---|---|---|---|---|---|---|---|
| G | Z0 | 0.597 | 0.027 | 0.427 | 4.081 | 0.102 | 1.22 | 1.00 |
| | Z1 | 0.633 | 0.025 | 0.461 | 3.531 | 0.131 | 1.19 | 0.99 |
| | Z2 | 0.622 | 0.012 | 0.453 | 6.194 | 0.075 | 1.19 | 0.99 |
| | Z5 | 0.627 | 0.011 | 0.472 | 9.045 | 0.064 | 1.15 | 0.98 |
| | Z10 | 0.627 | 0.009 | 0.506 | 15.679 | 0.035 | 1.16 | 0.97 |
| M | Z0 | 0.620 | 0.080 | 0.449 | 3.304 | 0.135 | 1.19 | 0.99 |
| | Z1 | 0.680 | 0.030 | 0.504 | 3.491 | 0.149 | 1.17 | 0.98 |
| | Z2 | 0.688 | 0.028 | 0.514 | 3.169 | 0.174 | 1.16 | 0.99 |
| | Z5 | 0.681 | 0.025 | 0.509 | 9.678 | 0.057 | 1.16 | 1.00 |
| | Z10 | 0.740 | 0.020 | 0.555 | 9.776 | 0.058 | 1.16 | 1.00 |
| R | Z0 | 0.494 | 0.040 | 0.372 | 4.815 | 0.120 | 1.15 | 0.98 |
| | Z1 | 0.502 | 0.014 | 0.386 | 5.325 | 0.125 | 1.13 | 0.98 |
| | Z2 | 0.504 | 0.012 | 0.390 | 8.813 | 0.080 | 1.13 | 0.97 |
| | Z5 | 0.533 | 0.017 | 0.414 | 9.567 | 0.076 | 1.12 | 0.97 |
| | Z10 | 0.540 | 0.017 | 0.416 | 25.387 | 0.027 | 1.13 | 0.94 |
| P | Z0 | 0.575 | 0.056 | 0.448 | 5.973 | 0.123 | 1.12 | 0.99 |
| | Z1 | 0.644 | 0.045 | 0.507 | 4.409 | 0.182 | 1.11 | 1.00 |
| | Z2 | 0.652 | 0.028 | 0.508 | 6.997 | 0.105 | 1.12 | 0.99 |
| | Z5 | 0.685 | 0.008 | 0.540 | 8.025 | 0.100 | 1.11 | 0.99 |
| | Z10 | 0.763 | 0.003 | 0.609 | 8.935 | 0.099 | 1.10 | 0.98 |

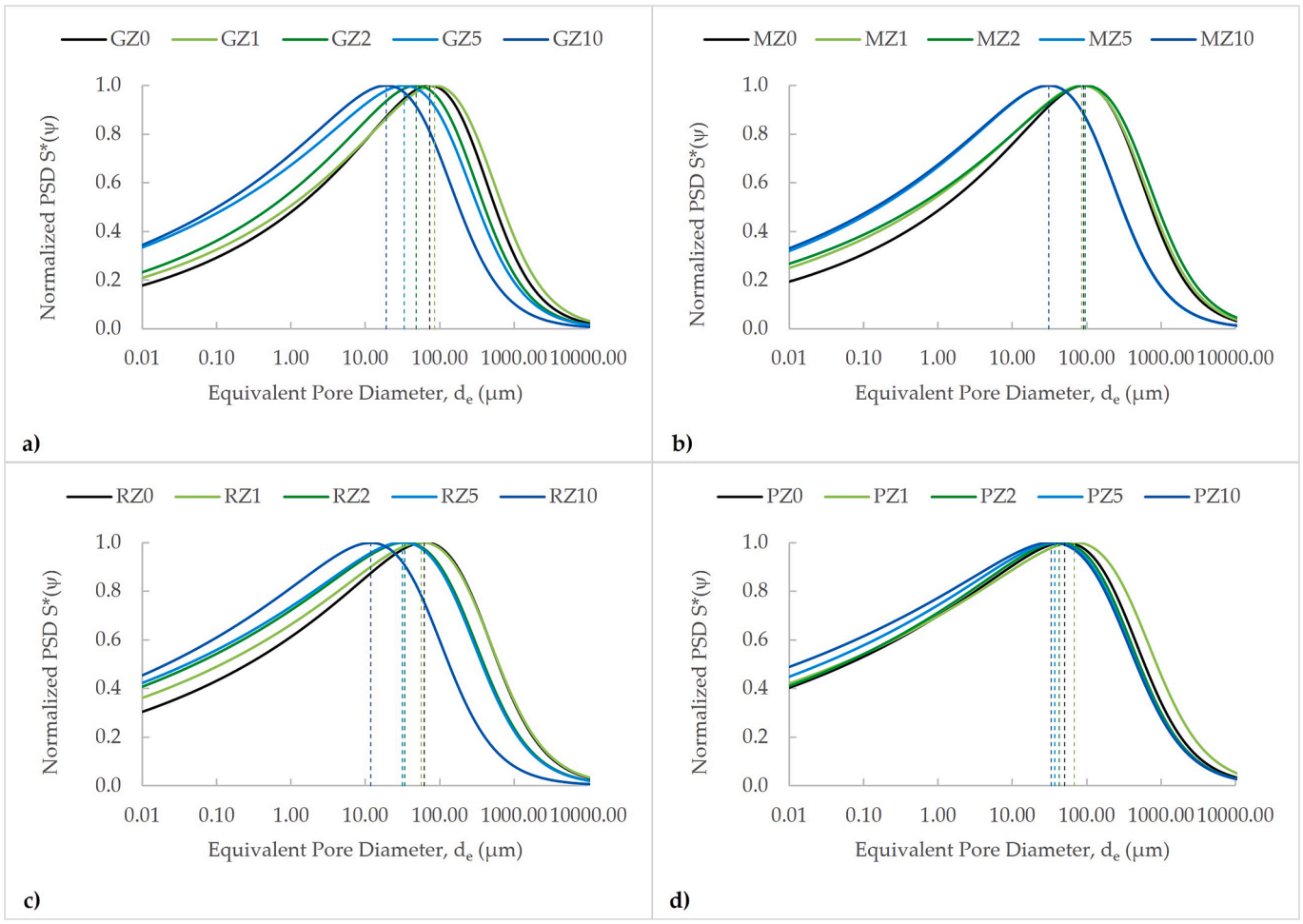


**Fig. 3.** Normalized pore size distribution functions S*(ψ) obtained using Eq. (2), as a function of equivalent pore diameter $d_e$ concerning the selected soils: a) Genzano (G), b) Metaponto (M), c) Rapolla (R), d) Pignola (P), and soil-zeolite mixtures (Z0, Z1, Z2, Z5, and Z10). Vertical dotted lines define the modal equivalent pore diameter, $d_{mode}$.

This reduction is less evident in the silty-loam soil of P. The standard deviation parameter (indicating the spread of the pore diameters) increases with the rise in the zeolite percentage. Notably, soils P and R exhibit higher SD values compared with soils G and M.

Furthermore, skewness and kurtosis parameters deviate from the ideal lognormal distribution. The negative skewness values increase (in absolute terms) in all soil combinations from Z0 to Z10, and a kurtosis value greater than 1 indicates a leptokurtic distribution, more peaked and tailed than the lognormal distribution. Volumes of macropores ($V_{mac} > 30$ μm; Cameron and Buchan, 2006; Fu et al., 2021) and micropores ($V_{mic} < 5$ μm) in soils G and M are similar in the absence of zeolite (i.e., in soil Z0). However, with an increase in zeolite amount, while $V_{mic}$ increases, $V_{mac}$ decreases. In soil P, a scenario of $V_{mic} \gg V_{mac}$ is observed initially, leading to a greater microporosity fraction in soils with Z10 without significant decreases in $V_{mac}$. Soil R exhibits a similar trend, positioning itself between soils G and M and soil P. Across all soils, the volume of mesopores ($5$ μm $< V_{mes} < 30$ μm) shows little variation with an increase in the zeolite percentage.

Going further into the analysis, the use of synthetic zeolite could be beneficial in coarse-textured soils, which typically have higher drainage porosity. In a study by Alessandrino et al. (2023), four soil conditioners, including a natural clinoptilolite-based zeolite, were compared. The study found that using this natural zeolite in three different soils, compared to the control, reduced drainage porosity while simultaneously increasing storage porosity (equivalent to the available water capacity, AWC), aligning with our findings. The results indicated that changes in soil physical quality indices were influenced not only by the zeolite's properties but also by the particle size and particle size distribution of the initial soil before the amendment was added. Therefore, the zeolite should only be used after testing it with the specific soil in question.

Table 4 lists the calculated soil parameters obtained using dynamic and static approaches. Overall, our observations indicate that, for a given soil type, all FCs and PWP values increase with increasing zeolite addition. $FC_{dyn}$, $FC_{AO}$ and $FC_{10}$ values clustered near the inflection point (refer also to Table 2), whereas $FC_{33}$ values are located near higher matric potential values, consequently displaying, on average, lower values. In particular, $FC_{10}$ and $FC_{33}$ values increased in the zeolite range Z0-Z10 up to 50 %, while $FC_{dyn}$ and $FC_{AO}$ values exhibited smaller increases (the increase ranged from about 10 % to 30 %).

This, in turn, affects the derived AWC values, albeit with smaller changes, due to the greater increase in PWP values as compared to FC, for a fixed soil and zeolite treatment. In particular, in G and M soils, PWP values, on average, increased (compared to Z0 reference) in the range of 20 % (Z1 treatments) up to 100 % (Z10 treatments). Finally, in R and P soils, these changes are of the order of 15 % (Z1 treatments) up to 60 % (Z10 treatments). This trend aligns with the findings by Villagra-Mendoza et al. (2021) and Zarebanadkouki et al. (2022). The variations caused by the addition of zeolite in soils influence the corresponding calculated RAWCs values.

**Table 3**
Location and shape parameters calculated from the PSD curves: modal ($d_{mode}$), median ($d_{median}$), and mean equivalent pore diameter ($d_{mean}$) values, standard deviation (SD), skewness (Skw), and kurtosis (Kurt), as well as the macroporosity ($V_{mac}$), mesoporosity ($V_{mes}$), and microporosity ($V_{mic}$) values as proposed by Reynolds et al. (2009) (In bold are the values within the optimal range).

| Soils | Zeolite | Location parameters | | | Shape parameters | | | $V_{mac}$ | $V_{mes}$ | $V_{mic}$ |
|---|---|---|---|---|---|---|---|---|---|---|
| | | $d_{mode}$ | $d_{median}$ | $d_{mean}$ | SD | Skw | Kurt | ($cm^3$ $cm^{-3}$) | | |
| | | (μm) | | | (−) | (−) | (−) | | | |
| G | Z0 | **73.5** | 12.4 | 5.3 | 71.0 | −0.380 | 1.149 | 0.238 | 0.113 | 0.246 |
| | Z1 | **85.0** | 10.7 | 4.1 | 114.2 | −0.393 | 1.146 | 0.250 | 0.110 | 0.274 |
| | Z2 | 48.4 | **6.2** | **2.3** | 112.8 | −0.392 | 1.146 | 0.205 | 0.118 | 0.299 |
| | Z5 | 33.2 | 2.0 | **0.6** | 352.4 | **−0.415** | **1.138** | 0.161 | 0.107 | 0.359 |
| | Z10 | 19.1 | 1.4 | **0.4** | 266.9 | **−0.411** | **1.140** | 0.139 | 0.124 | 0.414 |
| M | Z0 | **90.8** | 12.7 | 5.0 | 96.6 | −0.388 | **1.147** | 0.254 | 0.109 | 0.258 |
| | Z1 | **85.9** | 7.6 | 2.5 | 199.6 | −0.405 | **1.142** | 0.253 | 0.110 | 0.317 |
| | Z2 | **94.7** | **6.9** | **2.1** | 271.4 | **−0.411** | **1.140** | 0.254 | 0.107 | 0.327 |
| | Z5 | 31.0 | 2.3 | **0.7** | 271.4 | **−0.411** | **1.140** | 0.174 | 0.121 | 0.386 |
| | Z10 | 30.7 | 2.0 | **0.6** | 314.7 | **−0.413** | **1.139** | 0.186 | 0.129 | 0.425 |
| R | Z0 | **62.3** | **3.8** | **1.1** | 349.4 | **−0.415** | **1.138** | 0.158 | 0.079 | 0.257 |
| | Z1 | 56.3 | 2.0 | 0.4 | **809.9** | **−0.426** | **1.133** | 0.145 | 0.074 | 0.283 |
| | Z2 | 34.0 | 0.9 | 0.2 | **1177.7** | **−0.430** | **1.131** | 0.119 | 0.074 | 0.310 |
| | Z5 | 31.4 | 0.7 | 0.1 | **1450.7** | **−0.432** | **1.130** | 0.121 | 0.077 | 0.335 |
| | Z10 | 11.8 | 0.4 | 0.1 | **978.0** | **−0.429** | **1.132** | 0.080 | 0.085 | 0.376 |
| P | Z0 | 50.2 | 1.1 | 0.2 | 1559.2 | **−0.433** | **1.129** | 0.152 | 0.080 | 0.343 |
| | Z1 | **68.0** | 1.0 | 0.2 | 2953.2 | −0.438 | **1.126** | 0.178 | 0.082 | 0.384 |
| | Z2 | 42.9 | 0.9 | 0.2 | 1559.2 | **−0.433** | **1.129** | 0.164 | 0.092 | 0.396 |
| | Z5 | 37.4 | 0.5 | 0.1 | 2953.2 | −0.438 | **1.126** | 0.157 | 0.092 | 0.436 |
| | Z10 | 33.6 | 0.3 | 0.1 | 6366.6 | −0.443 | **1.123** | 0.161 | 0.096 | 0.507 |
| *Optimal Range* Reynolds et al. (2009) | | ***60–140*** | ***3–7*** | ***0.7–2*** | ***400–1000*** | ***−0.43to − 0.41*** | ***1.13–1.14*** | | | |

**Table 4**
Field capacity (FC), permanent wilting point (PWP), available water content (AWC) and readily available water content (RAWC) values calculated using dynamic and static criteria. For a fixed soil, mean values (n = 3) within a column followed by the same letter are not significantly different ($p \leq 0.05$) using Tukey's post-hoc test.

| soils | Zeolite | $FC_{dyn}$ | $FC_{AO}$ | $FC_{10}$ | $FC_{33}$ | PWP | $AWC_{dyn}$ | $AWC_{AO}$ | $AWC_{10}$ | $AWC_{33}$ | $RAWC_{dyn}$ | $RAWC_{AO}$ | $RAWC_{10}$ | $RAWC_{33}$ |
|---|---|---|---|---|---|---|---|---|---|---|---|---|---|---|
| G | Z0 | 0.392 | 0.379 | 0.358 | 0.279 | 0.123 | $0.269^{a}$ | 0.256 | $0.235^{a}$ | 0.156 | $0.171^{a}$ | 0.159 | 0.138 | $0.059^{a}$ |
| | Z1 | $0.435^{a}$ | 0.416 | 0.383 | 0.307 | 0.148 | $0.287^{b}$ | 0.269 | $0.236^{a}$ | 0.159 | 0.187 | 0.168 | $0.135^{a}$ | $0.058^{a}$ |
| | Z2 | $0.442^{a}$ | 0.409 | 0.417 | 0.335 | 0.161 | $0.280^{b}$ | 0.248 | 0.256 | $0.174^{a}$ | $0.170^{a}$ | 0.138 | 0.146 | 0.064 |
| | Z5 | 0.478 | 0.438 | 0.466 | 0.392 | 0.220 | 0.257 | $0.218^{a}$ | 0.245 | $0.172^{a}$ | 0.145 | 0.106 | $0.133^{a}$ | 0.060 |
| | Z10 | 0.514 | 0.467 | 0.538 | 0.454 | 0.248 | $0.266^{a}$ | $0.220^{a}$ | 0.290 | 0.206 | 0.132 | 0.085 | 0.156 | 0.072 |
| M | Z0 | 0.398 | 0.403 | 0.366 | 0.290 | 0.136 | $0.262^{a}$ | 0.268 | 0.231 | 0.155 | 0.165 | $0.170^{a}$ | $0.133^{a}$ | 0.057 |
| | Z1 | 0.483 | 0.462 | 0.427 | 0.350 | 0.183 | $0.299^{b}$ | $0.279^{a}$ | 0.244 | 0.167 | 0.192 | $0.172^{a}$ | 0.137 | 0.060 |
| | Z2 | $0.499^{a}$ | $0.475^{a}$ | 0.433 | 0.359 | 0.195 | $0.304^{b}$ | $0.280^{a}$ | 0.238 | 0.164 | 0.198 | 0.174 | $0.132^{a}$ | 0.058 |
| | Z5 | $0.496^{a}$ | $0.470^{a}$ | 0.506 | 0.424 | 0.231 | $0.265^{a}$ | 0.239 | 0.275 | 0.193 | 0.140 | 0.114 | 0.150 | 0.068 |
| | Z10 | 0.548 | 0.514 | 0.553 | 0.465 | 0.258 | $0.304^{b}$ | 0.256 | 0.295 | 0.207 | 0.170 | 0.122 | 0.161 | 0.072 |
| R | Z0 | 0.359 | 0.345 | 0.336 | 0.281 | 0.157 | 0.201 | 0.188 | $0.178^{a}$ | 0.124 | 0.121 | 0.107 | $0.098^{b}$ | 0.043 |
| | Z1 | 0.392 | $0.363^{b}$ | 0.357 | 0.306 | 0.185 | 0.207 | 0.178 | 0.172 | 0.121 | 0.128 | 0.098 | $0.092^{a}$ | 0.041 |
| | Z2 | 0.401 | $0.369^{b}$ | 0.384 | 0.334 | 0.208 | $0.193^{a}$ | 0.161 | $0.177^{a}$ | 0.126 | $0.110^{a}$ | $0.078^{a}$ | $0.093^{a}$ | 0.043 |
| | Z5 | $0.422^{a}$ | $0.393^{a}$ | 0.412 | 0.360 | 0.227 | $0.195^{a}$ | 0.166 | 0.185 | 0.133 | $0.107^{a}$ | $0.078^{a}$ | $0.097^{b}$ | 0.045 |
| | Z10 | $0.423^{a}$ | $0.393^{a}$ | 0.460 | 0.404 | 0.250 | 0.173 | 0.143 | 0.211 | 0.154 | 0.070 | 0.040 | 0.108 | 0.051 |
| P | Z0 | 0.441 | 0.425 | 0.423 | 0.368 | 0.233 | 0.208 | 0.191 | 0.190 | 0.135 | 0.118 | $0.102^{a}$ | 0.100 | 0.045 |
| | Z1 | $0.507^{a}$ | $0.484^{a}$ | 0.466 | 0.410 | $0.270^{a}$ | $0.238^{a}$ | $0.215^{bc}$ | 0.197 | 0.140 | 0.144 | 0.121 | 0.103 | 0.047 |
| | Z2 | $0.511^{a}$ | $0.482^{a}$ | 0.488 | 0.425 | $0.270^{a}$ | $0.241^{a}$ | $0.212^{ab}$ | $0.219^{a}$ | 0.156 | 0.138 | 0.109 | $0.115^{a}$ | $0.052^{a}$ |
| | Z5 | 0.566 | 0.515 | 0.528 | 0.466 | 0.307 | 0.259 | $0.209^{a}$ | $0.221^{a}$ | 0.159 | 0.153 | $0.103^{a}$ | $0.115^{a}$ | $0.053^{a}$ |
| | Z10 | 0.655 | 0.584 | 0.602 | 0.537 | 0.368 | 0.288 | $0.217^{c}$ | 0.235 | 0.170 | 0.174 | $0.103^{a}$ | 0.121 | 0.056 |

Table 5 shows the $E_I$ values calculated at different AWC and RAWC values. In most cases in the range Z0-Z10 $E_I$ values increase with increasing zeolite addition (this is always true in the Z0-Z2 domain). This aspect implies an increasing energy expenditure by plants, for water absorption from the soil, as the amount of zeolite increases. This is in agreement with Zarebanadkouki et al. (2022) who observed that the addition of silica and zeolite in a sandy soil increased the $E_I$ values. Particularly, high $E_I$ values were noted in soils containing 5 % and 10 % of zeolite.

On average, greater increases were observable for $E_I[\theta_{AWCdyn}]$ and $E_I[\theta_{RAWCAO}]$ values, where differences between Z0 and Z10 treatments are of the order of 30–40 %. In general, for $E_I[\theta_{AWCAO}]$ and $E_I[\theta_{RAWCAO}]$ values, the differences between Z0, Z1 and Z2 treatments were found to be statistically significant.

The changes in the FC and AWC values for the Basilicata soils are described in Fig. 4a and b. In all soils, a narrow interquartile range, representing low variability, was observed with the FC values calculated with dynamic criteria. The widest interquartile values were found in the FC values calculated with static criteria, while in soil P this also holds for the $FC_{dyn}$ value. With regard to parameter AWC, the highest values are observed in soils G and M. The variability of these values was high and the gap between $FC_{dyn}$, $FC_{AO}$, $FC_{10}$, and $FC_{33}$ values is more evident.

The graphs in Fig. 4c and d illustrate changes in $E_I$ values, across soils, for the different calculated AWC and RAWC parameters. As regards AWCs, the $E_I$ values of soils G and M are quite similar whereas higher values of $E_I$ are observed in R and P soils. As reported by Asgarzadeh et al. (2011) and Katigari et al. (2022), these values were caused by the greater reduction in pore diameter in the two soils (Fig. 3 and Table 3). $E_I$ values for $AWC_{AO}$ and $RAWC_{AO}$ showed the greatest variability.

Fig. 5 illustrates, among soils and zeolite treatments, the $E_I$ trend as a

**Table 5**
Integral energy $E_I$ (Joule $kg^{-1}$) mean values calculated at different available water and readily available water contents (AWC and RAWC) according to the dynamic and static approaches. For a fixed soil, mean values (n = 3) within a column followed by the same letter are not significantly different ($p \leq 0.05$) using Tukey's post-hoc test.

| Soils | Zeolite treatment | $E_I$ [$\theta_{AWCdyn}$] | $E_I$ [$\theta_{AWCAO}$] | $E_I$ [$\theta_{AWC10}$] | $E_I$ [$\theta_{AWC33}$] | $E_I$ [$\theta_{RAWCdyn}$] | $E_I$ [$\theta_{RAWCAO}$] | $E_I$ [$\theta_{RAWC10}$] | $E_I$ [$\theta_{RAWC33}$] |
|---|---|---|---|---|---|---|---|---|---|
| G | Z0 | 185.24$^{a}$ | 193.81$^{a}$ | 210.33 | 307.69 | 30.60 | 32.43 | 36.04$^{b}$ | 59.22$^{b}$ |
| | Z1 | 180.72$^{a}$ | 192.65$^{a}$ | 218.77$^{b}$ | 315.16$^{b}$ | 28.21 | 30.67 | 36.27$^{ab}$ | 59.12$^{b}$ |
| | Z2 | 202.95 | 228.74 | 221.92$^{b}$ | 318.12$^{b}$ | 32.46 | 38.08 | 36.57$^{a}$ | 59.41$^{ab}$ |
| | Z5 | 226.20 | 264.93 | 237.12$^{a}$ | 329.05$^{a}$ | 35.03 | 43.77 | 37.43 | 59.53$^{ab}$ |
| | Z10 | 258.26 | 309.31 | 238.11$^{a}$ | 328.36$^{a}$ | 42.54 | 55.01 | 37.89 | 59.89$^{a}$ |
| M | Z0 | 189.54 | 185.89 | 214.63 | 311.19 | 30.81 | 30.04 | 36.24 | 59.28$^{a}$ |
| | Z1 | 186.34 | 199.53 | 227.02$^{b}$ | 323.55$^{b}$ | 28.13 | 30.83 | 36.69$^{b}$ | 59.64$^{a}$ |
| | Z2 | 181.20 | 195.74 | 228.74$^{b}$ | 323.60$^{b}$ | 26.75 | 29.67 | 36.68$^{b}$ | 59.32$^{a}$ |
| | Z5 | 243.02$^{a}$ | 267.62$^{a}$ | 234.29$^{a}$ | 326.78$^{ab}$ | 39.33 | 45.03a | 37.37$^{a}$ | 59.65$^{a}$ |
| | Z10 | 241.51$^{a}$ | 270.73$^{a}$ | 236.74$^{a}$ | 329.96$^{a}$ | 38.42 | 45.02a | 37.25$^{a}$ | 59.59$^{a}$ |
| R | Z0 | 206.69$^{a}$ | 220.87 | 232.36 | 325.88 | 31.36 | 34.36 | 36.86$^{a}$ | 59.24$^{b}$ |
| | Z1 | 203.04$^{a}$ | 235.98 | 243.25$^{c}$ | 337.53$^{a}$ | 28.74 | 35.54 | 37.11$^{b}$ | 59.47$^{b}$ |
| | Z2 | 226.35 | 270.31 | 247.31$^{bc}$ | 339.06$^{a}$ | 33.17 | 42.89 | 37.70$^{a}$ | 59.76$^{ab}$ |
| | Z5 | 237.27 | 277.95 | 249.74$^{ab}$ | 341.29$^{a}$ | 35.07 | 44.18 | 37.78$^{a}$ | 59.77$^{ab}$ |
| | Z10 | 307.22 | 364.66 | 255.60$^{a}$ | 341.31$^{a}$ | 51.33 | 66.33 | 38.92 | 60.09$^{a}$ |
| P | Z0 | 227.35$^{a}$ | 246.06 | 247.72$^{b}$ | 340.89$^{b}$ | 33.18$^{a}$ | 37.18 | 37.54$^{ab}$ | 59.85$^{a}$ |
| | Z1 | 209.43$^{b}$ | 230.95 | 251.33$^{b}$ | 344.19$^{ab}$ | 28.80$^{b}$ | 33.14 | 37.47$^{b}$ | 59.60$^{a}$ |
| | Z2 | 226.13$^{a}$ | 255.65 | 248.37$^{b}$ | 340.48$^{b}$ | 32.99$^{a}$ | 39.38 | 37.76$^{ab}$ | 59.90$^{a}$ |
| | Z5 | 216.51 | 267.09 | 252.45$^{ab}$ | 343.92$^{ab}$ | 30.08 | 40.91 | 37.61$^{ab}$ | 59.58$^{a}$ |
| | Z10 | 210.73$^{b}$ | 277.22 | 256.86$^{a}$ | 347.93$^{a}$ | 28.34$^{b}$ | 42.54 | 37.96$^{a}$ | 59.90$^{a}$ |

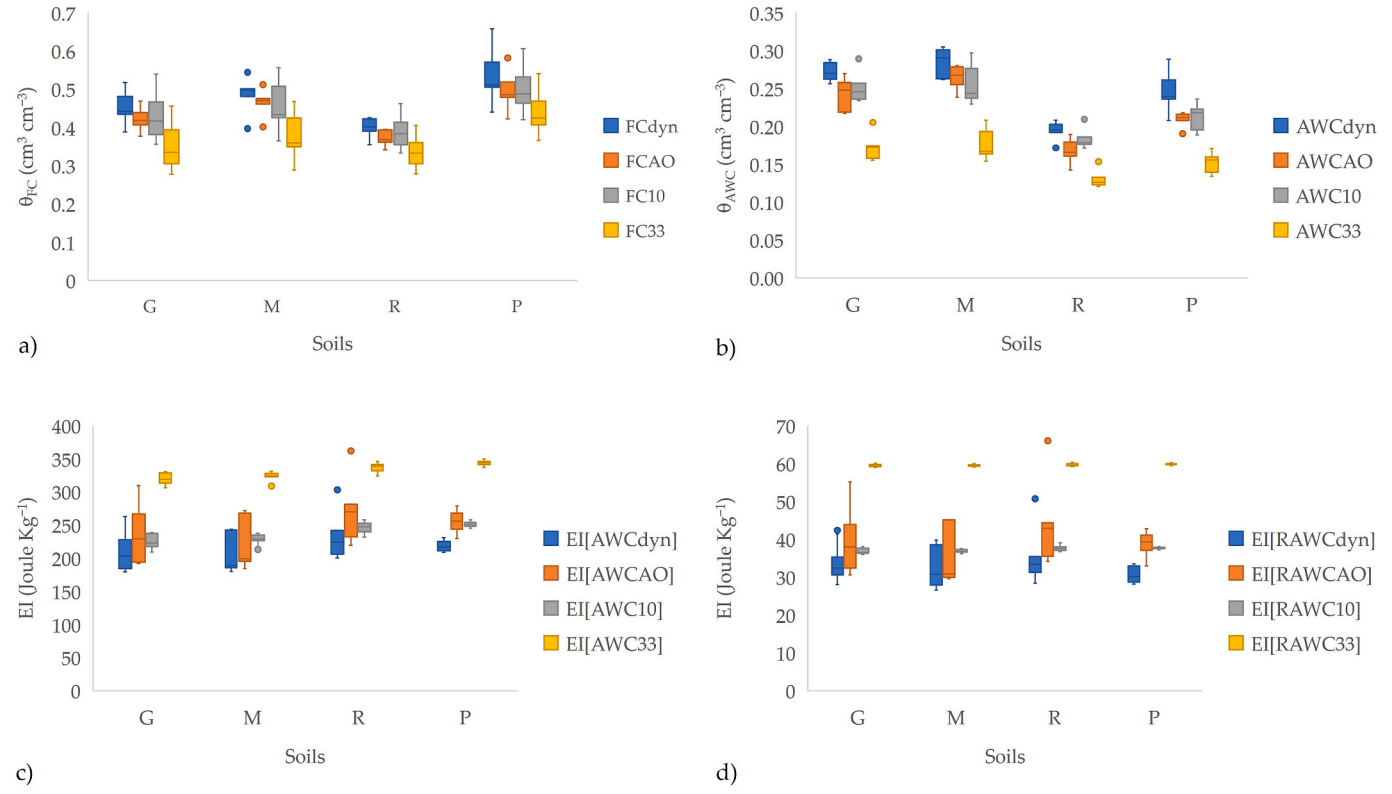


**Fig. 4.** a, b) Volumetric water content (θ) calculated at different field capacity (FC) and available water contents (AWC), and c, d) Integral Energy ($E_I$) values calculated at different AWC and readily available water contents (RAWC), as a function of the selected soil. The number of samples in each box = 15. The lower value of the box indicates the 25th percentile, the black line is the median and the higher bar value indicates the 75th percentile; whiskers indicate the 5th and 95th percentiles. Outliers are represented by solid circles beyond the whiskers.

function of AWC. Note that $E_I[AWC_{33}]$ values are consistently greater than those derived from $E_I[AWC_{dyn}]$, $E_I[AWC_{AO}]$, and $E_I[AWC_{10}]$ in all combinations except the case of GZ10 and RZ10, where $E_I[AWC_{AO}]$ demonstrated the opposite behavior, converging and overlapping with the trend of $E_I[AWC_{33}]$. Two or more soils, despite having different SWRCs, can have approximately identical AWC. The Integral Energy index that quantifies the energy applied by the soil to hold water in its pore between $\theta_{FC}$ and $\theta_{WP}$, can provide information, through the change in soil behavior (different SWRCs) before and after the addition of the different zeolite percentages, about the effect of the dosage on the management of the irrigation schedule. A plant cultivated on soils with a lower zeolite percentage (1 and 2 %) spends little energy taking up the same relative fraction of AWC compared to its cultivation in the same soil but with a higher zeolite percentage. This also means that, in soils

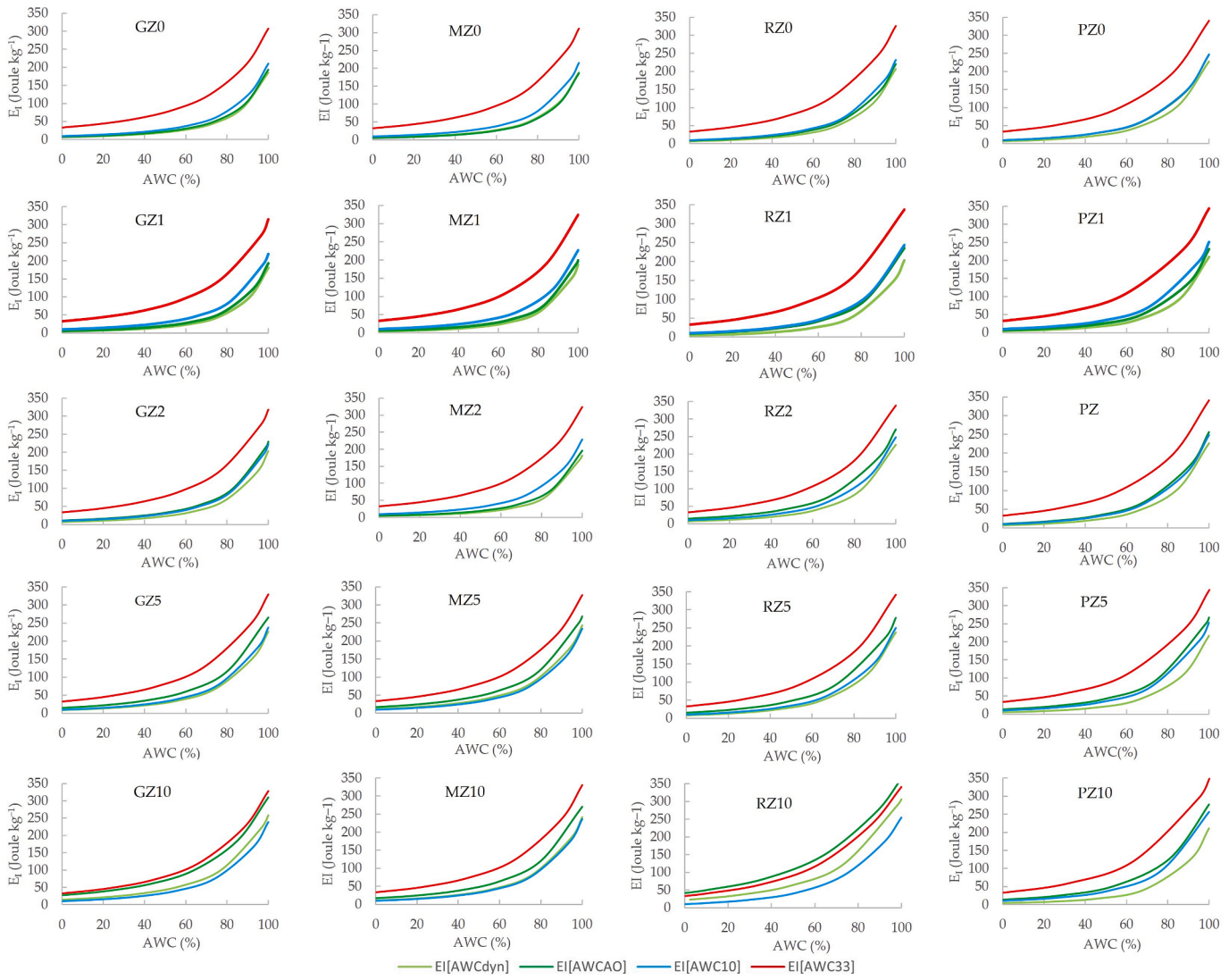


**Fig. 5.** $E_I$ values as a function of available water content (AWC) values for the different soil-zeolite mixtures.

with a higher zeolite dose (5 and 10 %), a closer irrigation cycle should be planned around a lower AWC consumption (20–30 %).

Fig. 6a, b, c, d, reports the stacked bar chart of the air capacity (AC) and relative field capacity (RFC) values for all soil-zeolite treatments. According to Reynolds et al. (2002), Reynolds et al. (2008), optimal soil aeration occurs when 66 % of the pore space is filled with water. Thus setting RFC to 0.66 and AC to 0.34 as optimal water and air content useful for plant and microbial activity, and considering the two dynamic criteria, it is evident that soils GZ0 and MZ0, unlike PZ0 and RZ0, were within this range. In all cases, zeolite addition increases RFC values (consequently reducing ACs).

Soil P (in all the explored situations) yielded the worst results for the two dynamic and static criteria. With respect to $FC_{33}$ values, there is an increase in the RFC index in soils G and M that is more evident than in soils R and P. In particular, at 2 % and 5 % of zeolite application, soils P and R were close to the optimum value.

### 3.2. Empirical relative field capacity (RFC) and integral energy ($E_I$) relationships

Through the experimental data of all soil-zeolite treatments, relationships among RFC as a function of macro-*meso*-microporosity ($V_{mac}$, $V_{mes}$, $V_{mic}$) and $E_I$ as a function of α and *n* vG parameters were determined, using a multiple stepwise linear regression analysis, and reported in Table 6.

Following equations 13–16, the micro-, meso-, and macroporosity account for 92 %, 98 %, and 99 % of the variability in RFC values. In the case of $RFC_{AO}$, the stepwise algorithm excluded $V_{mac}$ because it was not statistically significant ($p = 0.08$). Bondi et al. (2022), using a compost amendment, observed in the obtained RFC linear regression a significant increase in RFC values with increasing the compost amount, this behaviour was attributed to an overall increase in micropores.

Regarding equations 17–20, the negative relationship between integral energy and vG shape parameters indicates that the decrease in *α* and *n* negatively impacts the plant's energy requirement to uptake water. These results are comparable with those of Minasny and McBratney (2003), Asgarzadeh et al. (2011), and Zarebanadkouki et al. (2022).

### 3.3. Multivariate analysis

Multivariate analysis was also performed to explore the possible groupings between the selected soils mixed with zeolite through the selected soil's physical parameters. PCA analysis identified two principal components (PCs) which were assumed as variables and implemented in the subsequent cluster analysis. $PC_1$ and $PC_2$ components explained 87.34 % of the total variance of the soil physical properties (Table 7).

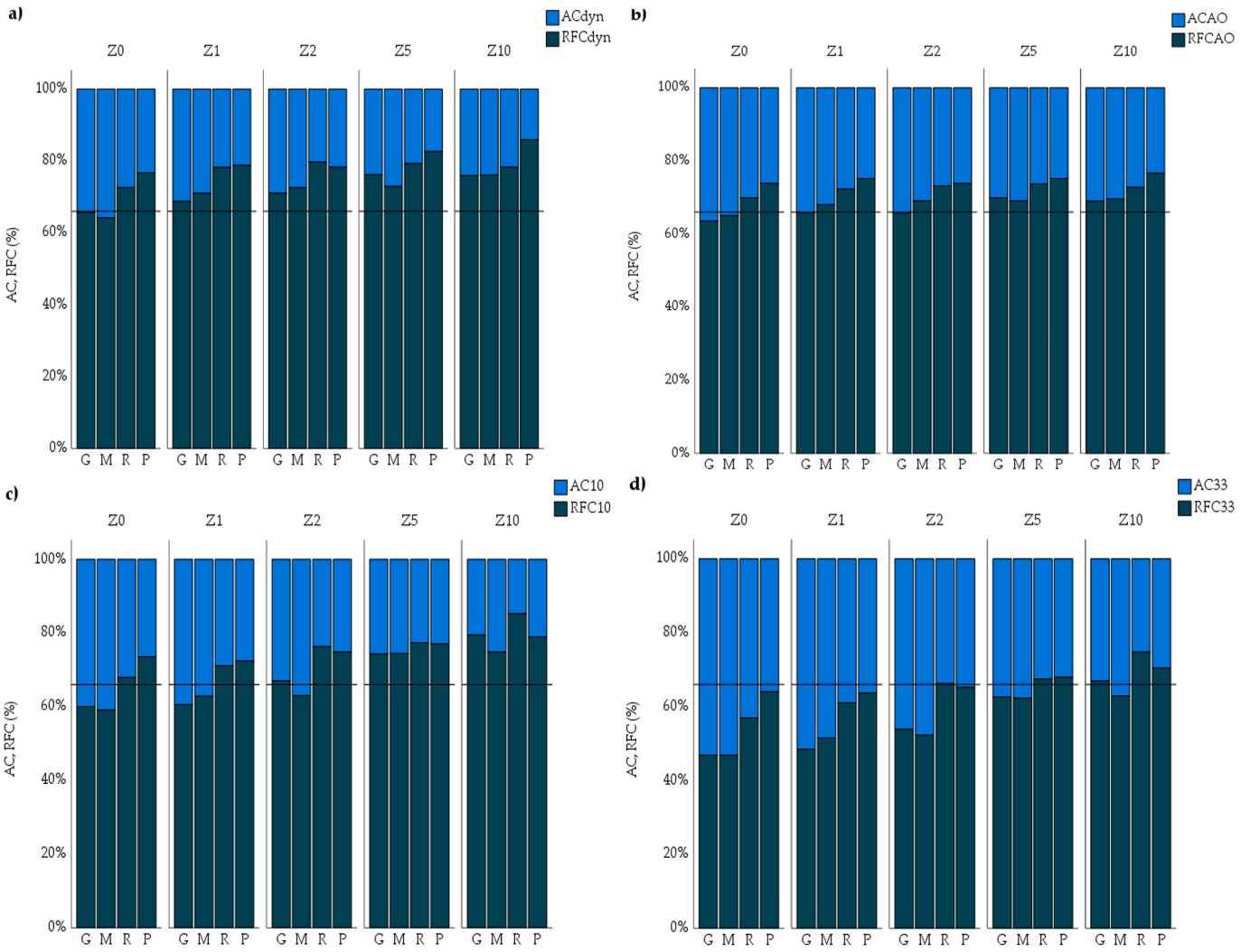


**Fig. 6.** Relative field capacity (RFC) and air capacity (AC) values for the different soil-zeolite mixtures obtained considering the four selected field capacity criteria (i.e., $FC_{dyn}$, $FC_{AO}$, $FC_{10}$, and $FC_{33}$). The horizontal solid lines represent the optimal value for the soil physical quality (SPQ) indicators (Reynolds et al., 2002; Reynolds et al., 2008).

**Table 6**
Multiple stepwise linear regression analysis of relative field capacity (RFC) and integral energy ($E_I$) parameters (all significant at $p < 0.001$).

| Equations | $R^2_{adjusted}$ | |
|---|---|---|
| $RFC_{dyn} = 0.738 + 0.574\ V_{mic} - 1.597\ V_{mes} - 0.156\ V_{mac}$ | 0.92 | (13) |
| $RFC_{AO} = 0.720 + 0.406\ V_{mic} - 0.468\ V_{mes}$ | 0.98 | (14) |
| $RFC_{10} = 0.743 + 0.405\ V_{mic} - 0.437\ V_{mes} - 1.189\ V_{mac}$ | 0.99 | (15) |
| $RFC_{33} = 0.641 + 0.570\ V_{mic} - 0.443\ V_{mes} - 1.059\ V_{mac}$ | 0.99 | (16) |
| $E_I[\theta_{AWCdyn}] = 703.31 - 551.885\ \alpha - 373.74n$ | 0.76 | (17) |
| $E_I[\theta_{AWCAO}] = 1170.448 - 800.924\ \alpha - 732.810n$ | 0.90 | (18) |
| $E_I[\theta_{AWC10}] = 714.181 - 62.240\ \alpha - 409.331n$ | 0.98 | (19) |
| $E_I[\theta_{AWC33}] = 739.152 - 25.053\ \alpha - 353.299n$ | 0.96 | (20) |

The $PC_1$ component describes 44 % of the total variance. The variables RFC (measured with dynamic FC criteria) and $E_I$ (measured with fixed FC criteria) gave the highest factor loading with a percentage of variance explained by $PC_1$ greater than 95 %. The $PC_2$ component describes 43 % of the total variance, and $d_{mode}$, $V_{mac}$, and $E_I$ (measured with dynamic FC criteria) gave the highest factor loading and a threshold of explained variance from the principal component extracted no less than 84 %.

The plot of the distribution of the variables under study is reported in Fig. 7a. Vectors pointing in similar directions indicate positively

**Table 7**
The first two independent principal component (PC) values and factor loadings obtained considering the four soils (G, M, R, and P) and the zeolite treatments (Z0, Z1, Z2, Z5, and Z10). The Kaiser-Meyer-Olkin (KMO) test ($p = 0.709$) and Bartlett's test of sphericity were adopted ($p < 0.001$) (components with an eigenvalue greater than or equal to 1 were selected).

| | $PC_1$ | $PC_2$ | |
|---|---|---|---|
| Initial eigenvalues | 9.02 | 1.45 | |
| % Variance explained | 75.21 | 12.13 | |
| % Cumulative variance explained | 75.21 | 87.34 | |
| Eigenvalues post rotation | 5.31 | 5.17 | |
| % Variance explained | 44.27 | 43.07 | |
| % Cumulative variance explained | 44.27 | 87.34 | |
| Variables | Factor loadings | | Communalities |
| $RFC_{dyn}$ | 0.903 | 0.379 | 0.960 |
| $RFC_{AO}$ | 0.969 | 0.208 | 0.983 |
| $RFC_{10}$ | 0.601 | 0.797 | 0.996 |
| $RFC_{33}$ | 0.710 | 0.700 | 0.995 |
| $d_{mode}$ | −0.324 | −0.917 | 0.946 |
| $V_{mac}$ | −0.505 | −0.765 | 0.841 |
| $V_{mic}$ | 0.658 | 0.404 | 0.596 |
| Ks | −0.220 | −0.540 | 0.340 |
| $E_I[\theta_{AWCdyn}]$ | 0.194 | 0.922 | 0.887 |
| $E_I[\theta_{AWCAO}]$ | 0.367 | 0.917 | 0.976 |
| $E_I[\theta_{AWC10}]$ | 0.894 | 0.426 | 0.981 |
| $E_I[\theta_{AWC33}]$ | 0.937 | 0.320 | 0.981 |

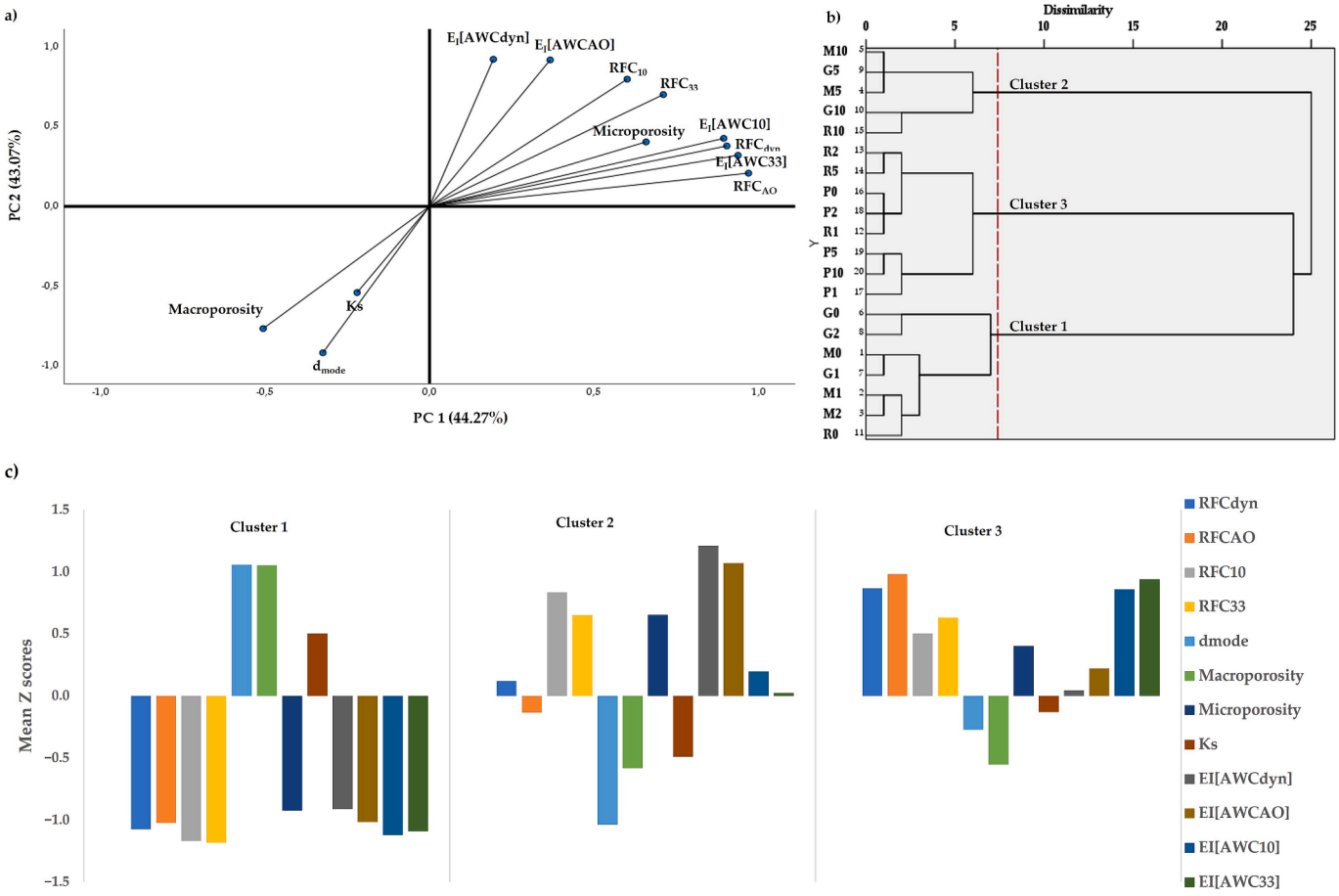


**Fig. 7.** a) Principal Component Analysis (PCA): plot showing the multivariate variation among soil-zeolite combination samples in terms of macroporosity, microporosity, modal equivalent diameter ($d_{mode}$), saturated hydraulic conductivity ($K_s$), and different relative field capacity (RFC) and integral energy ($E_I[\theta_{AWC}]$) calculated in accordance with dynamic and static field capacity. Vectors (lines) indicate the direction and strength of each variable to each principal component (PC1 and PC2), b) result of hierarchical cluster analysis, where the different combinations of letters (M, G, R, and P) and numbers (0, 1, 2, 5, and 10) express the type of soil and the dosage of zeolite applied in the soil + zeolite mixture and c) bar graph of *K*-means cluster analysis results of the three clusters.

**Table 8**
Pearson correlation coefficients between different relative field capacity (RFC), modal pore diameter ($d_{mode}$), macroporosity ($V_{mac}$) and microporosity ($V_{mic}$), saturated hydraulic conductivity ($K_s$), and different integral energy ($E_I$).

| | $RFC_{dyn}$ | $RFC_{AO}$ | $RFC_{10}$ | $RFC_{33}$ | $d_{mode}$ | $V_{mac}$ | $V_{mic}$ | $K_s$ | $E_I[\theta_{AWCdyn}]$ | $E_I[\theta_{AWCAO}]$ | $E_I[\theta_{AWC10}]$ |
|---|---|---|---|---|---|---|---|---|---|---|---|
| $RFC_{AO}$ | 0.944** | | | | | | | | | | |
| $RFC_{10}$ | 0.825** | 0.749** | | | | | | | | | |
| $RFC_{33}$ | 0.888** | 0.840** | 0.988** | | | | | | | | |
| $d_m$ | −0.638** | −0.498** | −0.926** | −0.867** | | | | | | | |
| $V_{mic}$ | 0.734** | 0.653** | 0.726** | 0.740** | −0.618** | −0.405** | | | | | |
| $K_s$ | −0.546** | −0.263* | −0.518** | −0.479** | 0.589** | 0.417** | −0.444** | | | | |
| $E_I[\theta_{AWCdyn}]$ | 0.443** | 0.400** | 0.862** | 0.801** | −0.865** | −0.814** | 0.480** | −0.300* | | | |
| $E_I[\theta_{AWCAO}]$ | 0.651** | 0.547** | 0.954** | 0.908** | −0.933** | −0.872** | 0.628** | −0.518** | 0.949** | | |
| $E_I[\theta_{AWC10}]$ | 0.945** | 0.965** | 0.873** | 0.935** | −0.656** | −0.808** | 0.693** | −0.355** | 0.600** | 0.727** | |
| $E_I[\theta_{AWC33}]$ | 0.940** | 0.974** | 0.806** | 0.881** | −0.578** | −0.745** | 0.666** | −0.321* | 0.499** | 0.634** | 0.988** |

†*Correlation is significant at the 0.05 level (2-tailed); **Correlation is significant at the 0.01 level (2-tailed).

correlated variables, and vectors pointing in opposite directions indicate negatively correlated variables. The angle between two vectors indicates their degree of correlation. The variables that are grouped on the positive quadrant between $PC_1$ and $PC_2$ are correlated significantly with each other, as are the variables grouped on the negative quadrant between $PC_1$ and $PC_2$. All the RFC and $E_I$ values were positively correlated ($p < 0.01$) with each other; $V_{mic}$ was also positively correlated ($p < 0.01$) with RFC and $E_I$. Conversely, $V_{mac}$, $K_s$, and $d_{mode}$ values were negatively correlated with RFC, $E_I$, and $V_{mic}$ (Table 8).

Cluster analysis using the two principal components ($PC_1$ and $PC_2$) as variables allowed us to identify the optimal number of clusters for the classification of soil-zeolite combinations (Fig. 7b). The cut on the dendrogram (indicated by the dotted line) which allowed the identification of the number of clusters was made before the value 10, which corresponded to the largest gap in the values of the distance coefficient between the 20 soil-zeolite combinations. Cluster 1 identifies the combinations of soils G and M without zeolite and with percentages of 1 % and 2 %. Also, soil R without zeolite is added to these soils. Cluster 2 groups the G and M soils in combination with 5 % and 10 % of zeolite, and soil R with 10 % of zeolite. In Cluster 3, soils P and R in combination with 1 %, 2 %, and 5 % of zeolite, were aggregated.

The clustered bar graph performed by non-hierarchical cluster analysis (K-means method) shows the differences in variables used in multivariate analysis (Fig. 7c). The preliminary ANOVA test indicated that $PC_1$ obtained a value of Fisher's *F* equal to 25.21, which is the one that significantly influenced the final composition of the clusters. $PC_2$ obtained a value of 16.6 of Fisher's *F*. Compared to the average levels in the total sample, Cluster 1 was differentiated from Cluster 2 and Cluster 3 by increased $d_{mode}$, $V_{mac}$, and $K_s$ values, and by decreased RFC, $E_I$, and $V_{mic}$. Cluster 2, compared to Cluster 3, has the lowest values of $d_{mode}$, $V_{mac}$, and $K_s$, and the highest $V_{mic}$, with respect to the average levels in the total sample.

## 4. Conclusions

In the current study, based on several laboratory experiments and hence on a full factorial database, we examined the effects of a synthetic zeolite on soil physical quality (SPQ) indicators across four soils with different pedological characteristics. The starting point of our analysis was field capacity, which is a recognized crucial parameter for effective soil water management practices and is essential for an adequate estimate of the above-mentioned soil physical quality indicators. The definition of field capacity is not universally agreed upon among researchers, and studies comparing the dynamic approach to the static one are limited. One advantage of Assouline and Or's (2014) model is that it determines the matric potential at field capacity using a simple analytical equation based on van Genuchten's parameters of the soil water retention curve.

As discussed in the paper, under a fixed criterion (static or dynamic), field capacity values varied, among soils, across the different zeolite treatments. With regard to the response of soil quality indicators, the Genzano and Metaponto soils in the cases of 1 % and 2 % zeolite percentages were closer to the reference values reported in the literature.

Moreover, the integral energy ($E_I$) approach provided valuable insights into soil water availability for plants. Our observations demonstrate that, in most cases, a decrease in soil pore diameter (due to zeolite addition) correlates with an increase in $E_I$ values.

From a textural point of view, we showed that the selected zeolite affects Genzano, Rapolla, and Metaponto soils (that are coarse-textured soils) rather than the soil at Pignola, which is a fine-textured. This aspect arises because the introduction of a finer fraction (i.e., zeolite) into coarse-textured soils may significantly alter their original pore size distribution, resulting in improved water retention capacity. However, all the observed peculiarities need to be further explored, as changes in soil pore size distribution can induce a sort of "clay-like" behavior that could be significant in agro-ecosystems. Nevertheless, this effect could be considered advantageous as it contributes to reducing the mobility of pesticides, nutrients, and other substances, but also of water. The observed increase in micropore volumes instead of macropores in soil-zeolite mixtures enables them to retain more water. However, this water is, on average, confined to narrower pathways, requiring plants to expend more energy to extract water from such smaller-radius pores.

In conclusion, the practice of amending soils with zeolites requires a rigorous approach, due to the complex correlations among the indicators of soil physical quality, that may be affected, among other things, by the zeolite nature, soil texture, and zeolite concentrations in soils. To confirm the observed effects of zeolites on soils, we believe that additional experiments and data sets are required on soils of different pedological contexts and textural characteristics, also employing different zeolites (i.e., synthetic and natural). Looking ahead, greenhouse and field-scale experiments should also be conducted to assess the observed effects on a scale of practical interest from an agronomic point of view, using an irrigation strategy aimed at controlling the water storage and soil-air capacity ratio.

## CRediT authorship contribution statement

**Antonio Satriani:** Writing – review & editing, Writing – original draft, Visualization, Validation, Methodology, Investigation, Formal analysis, Data curation, Conceptualization. **Claudia Belviso:** Writing – review & editing, Visualization, Validation, Methodology, Investigation, Conceptualization. **Stella Lovelli:** Writing – review & editing, Visualization, Validation, Methodology, Investigation, Conceptualization. **Simone di Prima:** Writing – review & editing, Investigation. **Antonio Coppola:** Writing – review & editing, Writing – original draft, Visualization, Validation, Methodology, Investigation, Formal analysis, Data curation, Conceptualization. **Shawkat B.M. Hassan:** Writing – review & editing, Investigation. **Anna Rita Rivelli:** Writing – review & editing, Investigation. **Alessandro Comegna:** Writing – review & editing, Writing – original draft, Visualization, Validation, Methodology, Investigation, Formal analysis, Data curation, Conceptualization.

## Declaration of competing interest

The authors declare that they have no known competing financial interests or personal relationships that could have appeared to influence the work reported in this paper.

## Appendix A. Supplementary data

Supplementary data to this article can be found online at https://doi.org/10.1016/j.geoderma.2024.117084.

## Data availability

Data will be made available on request.

## References

Ahuja, L.R., Nachabe, M.H., Rockiki, R., 2008. Soils: field capacity. In: Trimble, S.W., Howell, T.A. (Eds.), Encyclopedia of Water Science. CRC Press, Boca Raton, Florida, USA, pp. 1128–1131.

Alessandrino, L., Pavlakis, C., Colombani, N., Mastrocicco, M., Aschonitis, V., 2023. Effects of graphene on soil water-retention curve, van Genuchten parameters, and soil pore size distribution—a comparison with traditional soil conditioners. Water 2023 (15), 1297. https://doi.org/10.3390/w15071297.

Asgarzadeh, H., Mosaddeghi, M.R., Mahboubi, A.A., Nosrati, A., Dexter, A.R., 2011. Integral energy of conventional available water, least limiting water range and integral water capacity for better characterization of water availability and soil physical quality. Geoderma 166, 34–42.

Asgarzadeh, H., Mosaddeghi, M.R., Dexter, A.R., Mahboubi, A.A., Neyshabouri, M.R., 2014. Determination of soil available water for plants: Consistency between laboratory and field measurements. Geoderma 226–227, 8–20.

Assouline, S., Or, D., 2014. The concept of field capacity revisited: defining intrinsic static and dynamic criteria for soil internal drainage dynamics. Water Resour. Res. 50 (6), 4787–4802.

Barati, S., Reza, V.M., Reza, M.M., Bassiri, M., 2015. Plant-available water and integral energy for *Medicago sativa* and *Bromus tomentellus* in texturally different soils. Arch. Agron. Soil Sci. 62, 69–91. https://doi.org/10.1080/03650340.2015.1037295.
Belviso, C., 2018. State-of-the-art applications of fly ash from coal and biomass: a focus on zeolite synthesis processes and issues. Prog. Energy Combust. Sci. 65, 109–135.
Belviso, C., Satriani, A., Lovelli, S., Comegna, A., Coppola, A., Dragonetti, G., Cavalcante, F., Rivelli, A.R., 2022. Impact of zeolite from coal fly ash on soil hydrophysical properties and plant growth. Agriculture 12, 356. https://doi.org/10.3390/agriculture12030356.
Blake, G.R., Hartge, K.H., 1986. Particle density. In: Klute, A. (Ed.), Methods of Soil Analysis, Part 1, second ed. American Society of Agronomy, Madison, WI, pp. 377–381.
Blott, S.J., Pye, K., 2001. Gradistat: a grain size distribution and statistics package for the analysis of unconsolidated sediments. Earth Surf. Process. Landforms 26, 1237–1248.
Bondi, C., Castellini, M., Iovino, M., 2022. Compost amendment impact on soil physical quality estimated from hysteretic water retention curve. Water 14, 1002. https://doi.org/10.3390/w14071002.
Cameron, K., Buchan, G., 2006. Porosity and pore size distribution. Encycl. Soil Sci. 2, 1350–1353.
Cataldo, E., Salvi, L., Paoli, F., Fucile, M., Masciandaro, G., Manzi, D., Masini, C.M., Mattii, G.B., 2021. Application of zeolites in agriculture and other potential uses: a review. Agronomy 11, 1547. https://doi.org/10.3390/AGRONOMY11081547.
Chamindu Deepagoda, T.K.K., Chen Lopez, J.C., Møldrup, P., De Jonge, L.W., Tuller, M., 2013. Integral parameters for characterizing water, energy, and aeration properties of soilless plant growth media. J. Hydrol. 502, 120–127.
Cobzaru, C., Inglezakis, V., 2012. Mathematical modeling of sorption process of Cu 2 ions on analcime and clinoptilolite. Environ. Eng. Manag. J. 11 (11).
Colman, E.A., 1947. A laboratory procedure for determining the field capacity of soils. Soil Sci. 63, 277–283.
Colombani, N., Mastrocicco, M., Di Giuseppe, D., Faccini, B., Coltorti, M., 2015. Batch and column experiments on nutrient leaching in soils amended with Italian natural zeolitites. Catena 127, 64–71.
Comegna, A., Coppola, A., Dragonetti, G., Severino, G., Sommella, A., Basile, A., 2013. Dielectric properties of a tilled sandy volcanic vesuvian soil with moderate andic features. Soil till. Res. 133, 93–100. https://doi.org/10.1016/j.still.2013.06.003.
Comegna, A., Belviso, C., Rivelli, A.R., Coppola, A., Dragonetti, G., Sobhani, A., di Prima, S., Satriani, A., Cavalcante, F., Lovelli, S., 2023. Analysis of critical water flow and solute transport parameters in different soils mixed with a synthetic zeolite. Catena 228, 107150. https://doi.org/10.1016/j.catena.2023.107150.
Coppola, A., 2000. Unimodal and bimodal descriptions of hydraulic properties for aggregated soils. Soil Sci. Soc. Am. J. 64, 1252–1262.
Coppola, A., Dragonetti, G., Sengouga, A., Lamaddalena, N., Comegna, A., Basile, A., Noviello, N., Nardella, L., 2019. Identifying optimal irrigation water needs at district scale by using a physically based agro-hydrological model. Water 11, 841. https://doi.org/10.3390/w11040841.
Dane, J.H., Hopmans, J.W., 2002. 3.3.2.2 Hanging Water Column. In: Methods of Soil Analysis. John Wiley & Sons Ltd, pp. 680–683. https://doi.org/10.2136/sssabookser5.4.c25.
Day, P.R., 1965. Particle fractionation and particle-size analysis. In: Black, C.A. (Ed.), Methods of Soil Analysis, Part 1. American Society of Agronomy, Madison, pp. 545–567.
Demitri, C., Scalera, F., Madaghiele, M., Sannino, A., Maffezzoli, A., 2013. Potential of cellulose-based superabsorbent hydrogels as water reservoir in agriculture. Int. J. Polym. Sci. 12, 435073.
Dexter, A.R., 1988. Advances in characterization of soil structure. Soil Till. Res. 11, 199–238.
Dexter, A.R., 2004. Soil physical quality: Part I. Theory, effects of soil texture, density, and organic matter, and effects on root growth. Geoderma 120, 201–214.
Dexter, A.R., Bird, N.R.A., 2001. Methods for predicting optimum and the range of water contents for tillage based on water retention curve. Soil Till. Res. 57, 203–212.
Dexter, A.R., Czyz, E.A., Richard, G., Reszkowska, A., 2008. A user-friendly water retention function that takes account of the textural and structural pore spaces in soil. Geoderma 143, 243–253.
Dirksen, C., Matula, S., 1994. Automatic atomized water spray system for soil hydraulic conductivity measurements. Soil Sci. Soc. Am. J. 58, 319–325.
dos Reis, A.M.H., Armindo, R.A., Pires, L.F., 2019. Physical assessment of a Haplohumox soil under integrated crop-livestock system. Soil Till. Res. 194, 104294. https://doi.org/10.1016/j.still.2019.104294.
Drewry, J.J., Cameron, K.C., Buchan, G.D., 2008. Pasture yield and soil physical property responses to soil compaction from treading and grazing — a review. Aust. J. Soil Res. 46, 237–256.
Durner, W., 1994. Hydraulic conductivity estimation for soils with heterogeneous pore structure. Water Resour. Res. 30, 211–223.
Eckert, D.J., 1988. Soil pH. In: Dahnke, W.C. (Ed.), Recommended chemical soil test procedures for the North Central Region. Fargo: North Dakota Agricultural Experiment Station Bulletin No. 221 (revised), 6-8.
Elliot, A.D., Zhang, D., 2005. Controlled release zeolite fertilisers: a value added product produced from fly ash.
Ferretti, G., Rosinger, C., Diaz-Pines, E., Faccini, B., Coltorti, M., Keiblinger, K.M., 2024. Soil quality increases with long-term chabazite-zeolite tuff amendments in arable and perennial cropping systems. J. Environ. Manage. 354, 120303. https://doi.org/10.1016/j.jenvman.2024.120303.
Fu, Z., Hu, W., Beare, M., Thomas, S., Carrick, S., Dando, J., Langer, S., Müller, K., Baird, D., Lilburne, L., 2021. Lan use on soil hydraulic properties and the contribution of soil organic carbon. J. Hydrol. 602, 126741. https://doi.org/10.1016/j.jhydrol.2021.126741.
Guber, A.K., Rawls, W.J., Shein, E.V., Pachepsky, Y.A., 2003. Effect of soil aggregate size distribution on water retention. Soil Sci. 168, 223–233.
Hillel, D., 1980. Fundamentals of Soil Physics. Academic Press, New York, USA.
Hillel, D., 1998. Environmental soil physics. Academic Press Inc., London, p. 771.
Houlbrooke, D.J., Laurenson, S., 2013. Effect of sheep and cattle treading damage on soil microporosity and soil water holding capacity. Agric. Water Manage. 121, 81–84. https://doi.org/10.1016/j.agwat.2013.01.010.
Ibrahim, H.M., Alghamdi, A.G., 2021. Effects of the particle size of clinoptilotite zeolite on water content and soil water storage in a loamy sand soil. Water 13, 607. https://doi.org/10.3390/w13050607.
IUSS Working Group WRB, 2006. World reference base for soil resources 2006. A framework for international classification, correlation and communication. 2nd ed. World Soil Resour. Rep. 103. FAO, Rome.
Jakkula, V.S., Wani, S.P., 2018. Zeolites: Potential soil amendments for improving nutrient and water use efficiency and agriculture productivity. Sci. Rev. Chem. Commun. 8, 119–126.
Jarosz, R., Szerement, J., Gondek, K., Mierzwa-Hersztek, M., 2022. The use of zeolites as an addition to fertilisers-a review. Catena 213, 106125. https://doi.org/10.1016/j.catena.2022.106125.
Jensen, J.L., Schjønning, P., Watts, C.W., Christensen, B.T., Munkholm, L.J., 2019. Soil water retention: uni-modal models of pore-size distribution neglect impacts of soil management. Soil Sci. Soc. Am. J. 83, 18–26.
Katigari, M.S., Shabanpour, M., Davatgar, N., Vazifehdoust, M., 2022. Evaluation of spatial variability of the integral energy of plant available water and its influential properties in paddy soil. Paddy Water Environ. 20, 265–276. https://doi.org/10.1007/s10333-022-00892-9.
Klute, A., Dirksen, C., 1986. Hydraulic conductivity and diffusivity: laboratory methods. In: A. Klute (Ed.). Methods of Soil Analysis. Part 1. Physical and Mineralogical Methods. SSA Book Series: 5.
Meyer, P.D., Gee, G.W., 1999. Flux-based estimation of field capacity. J. Geotech. Geoenviron. Eng. 125, 595–599.
Minasny, B., McBratney, A.B., 2003. Integral energy as a measure of soil-water availability. Plant Soil. 249, 253–262.
Mohawesh, O., Durner, W., 2019. Effects of bentonite, hydrogel and biochar amendments on soil hydraulic properties from saturation to oven dryness. Pedosphere 29 (5), 598–607.
Mueller, L., Kay, B.D., Been, B., Hu, C., Zhang, Y., Wolff, M., Eulenstein, F., Schindler, U., 2008. Visual assessment of soil structure: Part II. Implications of tillage, rotation and traffic on sites in Canada, China and Germany. Soil Till. Res. 188–196.
Nakhli, S.A.A., Delkash, M., Bakhshayesh, B.E., Kazemian, H., 2017. Application of zeolites for sustainable agriculture: a review on water and nutrient retention. Water Air Soil Pollut. 228. https://doi.org/10.1007/s11270-017-3649-1.
Nasta, P., Franz, T.E., Gibson, J.P., Romano, N., 2023. Revisiting the definition of field capacity as a functional parameter in a layered agronomic soil profile beneath irrigated maize. Agric. Water Manag. 284, 108368. https://doi.org/10.1016/j.agwat.2023.108368.
Ndung'u, M., Ngatia, L.W., Onwonga, R.N., Mucheru-Muna, M.W., Fu, R., Moriasi, D.N., Ngetich, K.F., 2021. The influence of organic and inorganic nutrient inputs on soil organic carbon functional groups content and maize yields. Heliyon 7 (8), e07881.
Novotny, E.H., Ribeiro deAzevedo, E., de Godoy, G., Martelozo Consalter, D., Cooper, M., 2023. Determination of soil pore size distribution and water retention curve by internal magnetic field modulation at low field H NMR. Geoderma 431, 116363.
Ravali, C., Rao, K.J., Anjaiah, T., Suresh, K., 2020. Effect of zeolite on soil physical and physico-chemical properties. Multilogic Sci. 10, 776–781.
Reynolds, W.D., Bowman, B.T., Drury, C.F., Tan, C.S., Lu, X., 2002. Indicators of good soil physical quality: density and storage parameters. Geoderma 110, 131–146.
Reynolds, W.D., Drury, C.F., Yang, X.M., Fox, C.A., Tan, C.S., Zhang, T.Q., 2007. Land management effects on the near-surface physical quality of a clay loam soil. Soil Till. Res. 96, 316–330.
Reynolds, W.D., Drury, C.F., Yang, X.M., Tan, C.S., 2008. Optimal soil physical quality inferred through structural regression and parameter interactions. Geoderma 146, 466–474.
Reynolds, W.D., Drury, C.F., Tan, C.S., Fox, C.A., Yang, X.M., 2009. Use of indicators and pore volume-function characteristics to quantify soil physical quality. Geoderma 152 (3–4), 252–263. https://doi.org/10.1016/j.geoderma.2009.06.009.
Richards, L.A., Weaver, L.R., 1944. Moisture retention by some irrigated soils as related to soil moisture tension. J. Agric. Res. 69, 215–235.
Field Water Capacity, in Methods of Soil Analysis: Part 4. Physical Methods, SSSA Book Ser vol. 5, 2002, 722–738.
Saha, A., Sekharan, S., Manna, U., 2020. Superabsorbent hydrogel (SAH) as a soil amendment for drought management: a review. Soil Tillage Res. 204, 104736. https://doi.org/10.1016/j.still.2020.104736.
Satriani, A., Catalano, M., Scalcione, E., 2018. The role of superabsorbent hydrogel in bean crop cultivation under deficit irrigation conditions: a case-study in Southern Italy. Agric. Water Manag. 195, 114–119.
Schaller, J., Cramer, A., Carminati, A., Zarebanadkouki, M., 2020. Biogenic amorphous silica as main driver for plant available water in soils. Sci. Rep. 10, 2424. https://doi.org/10.1038/s41598-020-59437-x.
Six, J., Conant, R., Paul, E.A., Paustian, K., 2002. Stabilization mechanisms of soil organic matter: implications for C-saturation of soils. Plant Soil 241, 155–176.
Stackman, W.P., Valk, G.A., van der Harst, G.G., 1969. Determination of soil moisture retention curves: I. Sand box apparatus. In: Range (Ed.). Wageningen, ICW, pp. 119.

Szatanik-Kloc, A., Szerement, J., Adamczuk, A., Jozefaciuk, G., 2021. Effect of low zeolite doses on plants and soil physicochemical properties. Mater. (Basel) 14, 1–18. https://doi.org/10.3390/ma14102617.

Szerement, J., Ambrozewich-Nita, A., Kedziora, K., et al., 2014. Use of zeolite in agriculture and environmental protection. A short review. UDC 666 (96–691), 54.

Topp, G.C., Reynolds, W.D., Cook, F.J., Kirby, J.M., Carter, M.R., 1997. Physical attributes of soil quality. In: Gregorich, E.G., Carter, M.R. (Eds.), Soil Quality for Crop Production and Ecosystem Health. in: Developments in Soil Science, vol. 25. Elsevier, New York, NY, pp. 21–58.

Twarakavi, N.K.C., Šimůnek, J., Schaap, M.G., 2009. Development of pedotransfer functions for estimation of soil hydraulic parameters using support vector machines. Soil Sci. Soc. Am. J. 73, 1443–1452.

van Genuchten, M.Th., 1980. A closed-form equation for predicting the hydraulic conductivity of unsaturated soils. Soil Sci. Soc. Am. J. 44, 892–898.

Van Genuchten, M.V., Leij, F.J., Yates, S.R., 1991. The RETC Code for Quantifying the Hydraulic Functions of Unsaturated Soils. Berlin, Germany, ResearchGate.

Veihmeyer, F.J., Hendrickson, A.H., 1927. Soil-moisture conditions in relation to plant growth. Plant Physiol. (Bethesda) 2 (1), 71–82.

Veihmeyer, F.J., Hendrickson, A.H., 1931. The moisture equivalent as a measure of the field capacity of soils. Soil Sci. 32, 181–193.

Villagra-Mendoza, K., Masís-Meléndez, F., Quesada-Kimsey, J., García-González, C.A., Horn, R., 2021. Physicochemical changes in loam soils amended with bamboo biochar and their influence in tomato production yield. Agronomy 11, 2052. https://doi.org/10.3390/agronomy11102052.

Zarebanadkouki, M., Hosseini, B., Gerke, H.H., Schaller, J., 2022. Amorphous silica amendment to improve sandy soils' hydraulic properties for sustained plant root access under drying conditions. Front. Environ. Sci. 10, 935012. https://doi.org/10.3389/fenvs.2022.935012.

Zheng, Q., Hu, Y., Zhang, S., Noll, L., Böckle, T., Dietrich, M., Herbold, C.W., Eichorst, S. A., Woebken, D., Richter, A., Wanek, W., 2019. Soil multifunctionality is affected by the soil environment and by microbial community composition and diversity. Soil Biol. Biochem. 136, 10752. https://doi.org/10.1016/j.soilbio.2019.107521.